Nanoarchitectures

DOI: 10.1002/anie.200702451

Facile Shape-Controlled Synthesis of Well-Aligned Nanowire Architectures in Binary Aqueous Solution**

*Xiao-Fang Shen and Xiu-Ping Yan**

Physical and chemical properties of nanomaterials depend not only on their composition but also on their structure, morphology, phase, shape, size, distribution, and spatial arrangement.[1] Architectural control of nanosized materials with well-defined shapes is significant for "bottom-up" approaches toward future nanodevices. Therefore, finding new ways to assemble nanoobjects into finite superstructures is an important task.

One-dimensional (1D) nanomaterials have attracted much attention because of their intriguing properties and potential applications.[2] The impact of aligned and arranged 1D nanomaterial patterns would be tremendous in many areas, from nanoscale electronics and optoelectronics to molecular sensing.[3] In recent years, various procedures including the logs-on-a-river or Langmuir–Blodgett technique[4] and microfluidic,[5] electrical,[6] nanoimprinting,[7] self-organization,[8] and electric-field-effect-based demultiplexing methods[9] have been developed to assemble 1D nanomaterials into ordered patterns. These thought-provoking works inspired us to explore a simple approach for the low-cost, large-scale, room-temperature, and controlled growth of well-arranged nanostructures at atmospheric pressure.

As a result of the special structures and fascinating self-assembling functions, a biomaterial-based templating technique for the synthesis and assembly of novel artificial nanostructures of crystalline inorganic materials has given a promising focus in the preparation of various nanostructures.[10] In particular, L-cysteine, a very important biomolecule with three functional groups (SH, NH_2, COOH), has a strong tendency to coordinate with inorganic cations and metals, and has been exploited in the synthesis of quantum dots,[11] nanotubes,[12] 3D spherical nanostructures from nanorods,[13] and flowerlike patterns with nanorods.[14]

Herein, we report the facile and shape-controlled synthesis of dandelion-like L-cysteine–Pb architectures assembled from well-aligned nanowires in a binary aqueous solution of L-cysteine and $Pb(OAc)_2$ at room temperature, and their evolution into spherical and various flowerlike PbS microstructures under conventional hydrothermal conditions.

Well-controlled complex morphologies are usually difficult to acquire by directly mixing two incompatible solutions because of the rapid decrease in supersaturation and further depletion of reaction nutrients in a short period of time.[15] However, we readily obtained well-organized, assembled nanowire architectures by injecting an aqueous solution of $Pb(OAc)_2$ (0.1 M, 0.25 mL) into an aqueous solution of L-cysteine (0.01 M, 2.5 mL) at room temperature. Investigation by scanning electron microscopy (SEM) proved the formation of a large quantity of uniform architectures (Figure 1a) assembled from well-aligned nanowires (Figure 1b). The reaction process was recorded by optical microscopy (see video in the Supporting Information).

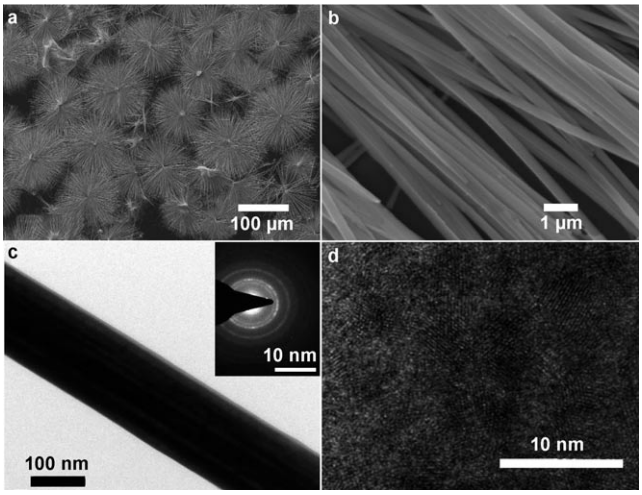

Figure 1. Characterization of L-cysteine–Pb nanoarchitectures prepared by injecting an aqueous solution of $Pb(OAc)_2$ (0.1 M, 0.25 mL) into an aqueous solution of L-cysteine (0.01 M, 2.5 mL). a) SEM image, b) high-resolution (HR) SEM image, c) TEM image, and d) HRTEM image. The inset in (c) shows the electron diffraction pattern of the nanowire.

To facilitate studies on the reactant concentration and the evolution of the morphology with time, the reaction was started with a medium concentration of building blocks (L-cysteine and $Pb(OAc)_2$, 4 mM; the SEM image of the corresponding final product is shown in Figure 2c). In the course of the reaction (50 min), the temporal evolution of the $Pb(OAc)_2$ concentration in the solution was monitored by flame atomic-absorption spectrometry (Supporting Information). The corresponding time-dependent evolution of the morphology of the products was recorded by transmission electron microscopy (TEM; see Supporting Information).

[*] X.-F. Shen, Prof. Dr. X.-P. Yan
Research Center for Analytical Sciences
College of Chemistry, Nankai University
Tianjin 300071 (P.R. China)
Fax: (+86) 22-2350-6075
E-mail: xpyan@nankai.edu.cn

[**] This work was supported by the National Basic Research Program of China (2006CB705703).

Supporting information for this article is available on the WWW under http://www.angewandte.org or from the author.

In the first 2.5 minutes of reaction, the concentration of $Pb(OAc)_2$ in the solution decreased to 3.75 mM, and nanorods about 30 nm in diameter and several hundreds of nanometers in length were formed. After five minutes of reaction, the concentration of $Pb(OAc)_2$ was depleted to 3.65 mM, and wirelike objects about 200 nm in diameter and several micrometers in length with branches on their tips were observed. The concentration of $Pb(OAc)_2$ in the solution further decreased to 3.54 mM, and more branches on the tips of the wirelike objects evolved. The depletion of the concentration of $Pb(OAc)_2$ in the last 30 minutes was much slower than that in the first 20 minutes. Finally, 3D highly branched spherical microstructures (dandelion-like L-cysteine–Pb architectures; Figure 2c) were formed. The above results indicate that a splitting growth mechanism was most likely responsible for the formation of the dandelion-like flowers, as in the case of the growth of Bi_2S_3.[16]

Generally speaking, crystal splitting is associated with fast crystal growth, which depends strongly on the oversaturation of the solution.[16] Variation in the concentration of the building blocks resulted in successive splitting of the L-cysteine–Pb nanoarchitectures (Figure 2a–f). As shown in Figure 2a, at low L-cysteine and $Pb(OAc)_2$ concentrations (0.8 mM each) shuttle-like fusiform bundles about 300 μm long were formed, with the nanowires showing slight splitting at both tips of the shuttles. As the concentration of the building blocks increased to 2 mM, nanowires developed out from the sides of the shuttle-like fusiform bundles, which made them look like butterflies (about 300 μm long) with spreading wings (Figure 2b). The imprints of the shuttles still remained in the main body of the butterflies. Then the bodies of the butterfly-like structures split intensively, the shuttle-like fusiform bundles disappeared, and the wings of the butterflies were unified. Thus, surprisingly, beautiful dandelion-like flowers (about 250 μm in diameter) consisting of well-aligned nanowires (Figure 2c) appeared. With a further increase in concentration of the building blocks, the branches of the dandelion-like flowers tended to grow much denser, and the diameter changed from ca. 130 (Figure 2d) to 80 (Figure 2e) and again to 130 μm (Figure 2f).

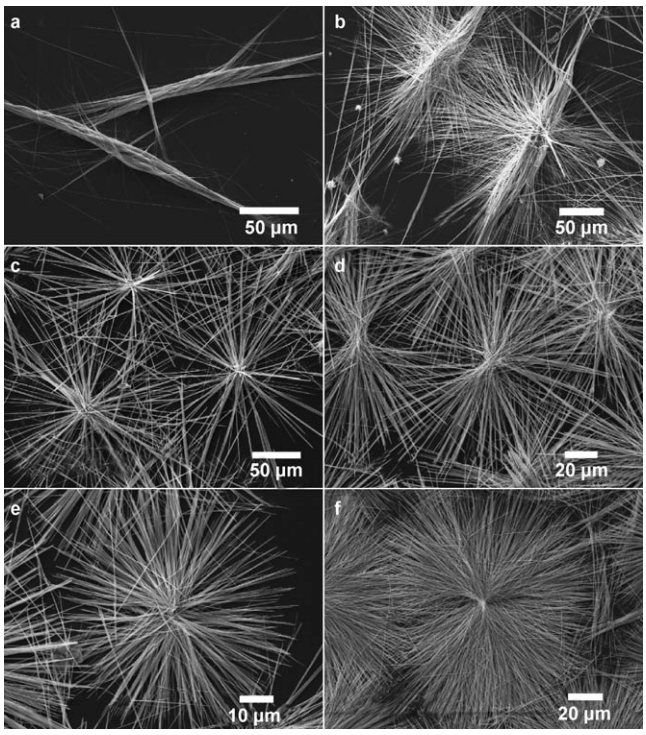

Figure 2. Representative low-magnification SEM images of L-cysteine–Pb nanoarchitectures prepared with L-cysteine and $Pb(OAc)_2$ concentrations of a) 0.8, b) 2, c) 4, d) 6, e) 7, and f) 9 mM each.

High-magnification SEM images of the nanoarchitectures (Figure 2a–f) revealed that the products were assemblies of homogeneous individual nanowires with narrow diameter distributions. There are several key characteristics that can be identified from the high-magnification SEM studies. First, the nanowires were well-arranged and appeared in a radiating form. Second, the nanowires were straight and their surfaces were very smooth. Third, the diameters of most nanowire branches did not change significantly in the same sample. However, over the course of the increase in concentration, the diameter increased from ca. 150 nm to 200 and 1000 nm, then decreased to 500, 200 and 150 nm (Supporting Information). Clearly, the morphology and size of the well-aligned L-cysteine–Pb nanowires were controllable by adjusting the concentration of the building blocks.

In addition to concentration, the molar ratios of the two building blocks in the binary solution also significantly influenced the morphology of the product (Figure 3a–d).

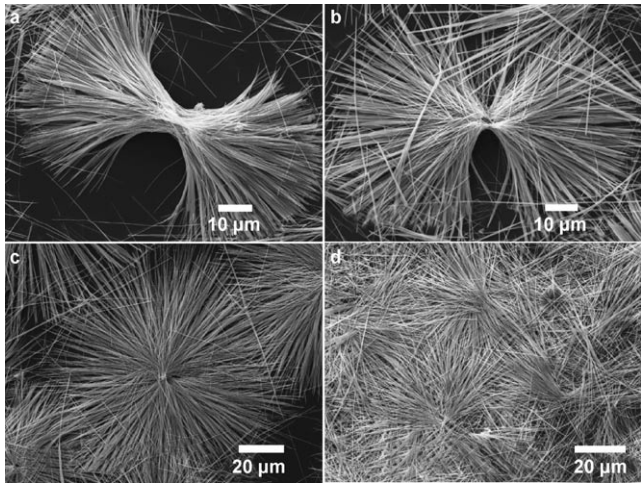

Figure 3. Low-magnification SEM images of L-cysteine–Pb nanoarchitectures prepared with various L-cysteine/$Pb(OAc)_2$ molar ratios: a) 4:1, b) 2:1, c) 1:1, d) 1:2.

Splitting of the nanoarchitectures was enhanced with decreasing L-cysteine/$Pb(OAc)_2$ molar ratio. At a molar ratio of 4:1, a dual fanlike architecture split out from the core (Figure 3a). Two fantails were banded together and fan blades radiated out in opposite directions. The dual fans were wider and the fantails became smaller when the molar ratio decreased to 2:1 (Figure 3b). On complete splitting out, the dual fans unified and dandelion-like flowers were obtained (Figure 3c) at the

molar ratio of 1:1. A molar ratio of 1:2 resulted in bundles of nanowires without conjugation, but the radiating trends of the architecture remained (Figure 3d) as a result of oversplitting during crystallization.

High-magnification SEM analysis of the conjugating parts of the architectures was expected to provide structural information on the mechanism of their formation (see Supporting Information). The conjugating parts of the samples were obtained at L-cysteine/$Pb(OAc)_2$ molar ratios of 4:1, 2:1, 1:1, and 1:2, respectively. Conjugates of the dual fans consisted of numerous nanowires with low splitting level. At molar ratios of 2:1 and 1:1, the core part was no longer whole and the linking nanowires in the cores were broken. The core finally disappeared, probably because of oversplitting during crystallization.

Surfactant has been widely employed as a soft template in the synthesis of inorganic nanostructures.[17] Herein, we also investigated the influence of surfactant on the morphological evolution of L-cysteine–Pb nanoarchitectures. Cetyltrimethylammonium bromide (CTAB) was used as a model surfactant. The morphology of L-cysteine–Pb nanoarchitectures changed strongly with the concentration of CTAB in the range of 0–2.0 mM (Figure 4a–d). In the absence of CTAB, dandelion-like flowers were obtained (Figure 4a). Addition of 1.0 mM CTAB prevented these architectures from splitting, and dual fanlike patterns formed (Figure 4b). The splitting was further held back and sisal-like structures were formed on increasing the concentration of CTAB to 1.5 mM (Figure 4c). The high-magnification SEM image of these structures (see Supporting Information) indicates that splitting was strongly inhibited and only slight splitting occurred at the tips. A further increase of the concentration of CTAB to 2.0 mM led to irregular nanowires (Figure 4d). The surfactant may change the initial speciation of L-cysteine and kinetically control the progress of splitting during growth. However, the exact role of CTAB in the growth of L-cysteine–Pb nanoarchitectures needs further investigation.

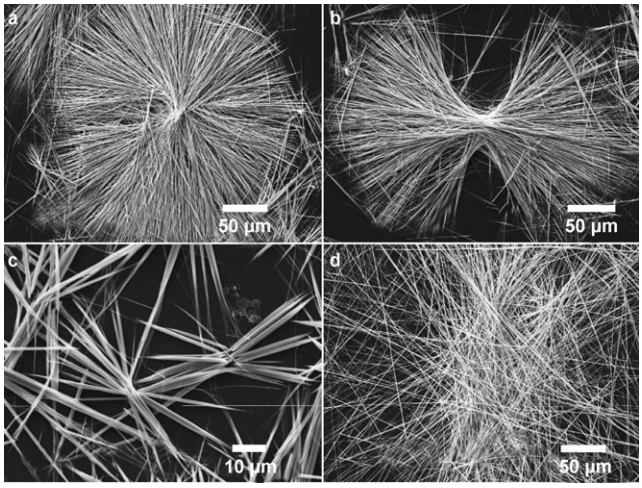

Figure 4. SEM images of L-cysteine–Pb nanoarchitectures assisted by various concentrations of CTAB [mM]: a) 0, b) 1.0, c) 1.5, d) 2.0. The concentrations of L-cysteine and $Pb(OAc)_2$ were both fixed at 9 mM.

The powder X-ray diffraction (PXRD) pattern of dandelion-like nanoarchitectures (see Supporting Information) shows that they were well-crystallized. The TEM image of a typical single nanowire (Figure 1c) reveals that it was straight and had a smooth surface. A representative HRTEM image (Figure 1d) of the nanowire and the electron diffraction pattern (inset in Figure 1c) indicate that the nanowire was polycrystallized and the size of the crystals was about 5 nm.

The Fourier-transform infrared (FTIR) spectrum of the as-prepared L-cysteine–Pb also provides preliminary proof of the intermolecular bonding (see Supporting Information). In comparison with the FTIR spectrum of pure L-cysteine, the characteristic bands of NH_3^+ at 2082 cm^{-1} and of SH at about 2552 cm^{-1} disappeared after binding with Pb. The bands at 1586 and 1545 cm^{-1} (attributed to the characteristic peaks of the I and II bands for amino acids) and at 3434 cm^{-1} (O–H stretching vibrations) did not shift significantly, which indicates that the COOH group did not participate in nanowire formation. Thus, the likely chemical structure of the dandelion-like flowers was $[\text{-S-CH}_2\text{CH(COOH)NH-Pb-}]_n$.

Interestingly, under conventional hydrothermal conditions, snow-white L-cysteine–Pb dandelion-like flowers assembled from well-aligned nanowires evolved into a black powder of micrometer-sized semiconductor PbS with attractive morphologies: microspheres, various flowers, and needles (Figure 5). PXRD patterns (Supporting Information) of the as-synthesized black products confirmed the formation of PbS crystallites of cubic phase (JCPDS Card File No. 05-0592). PbS microspheres were formed by directly decomposing L-cysteine–Pb dandelion-like flowers in pure water. The micro-

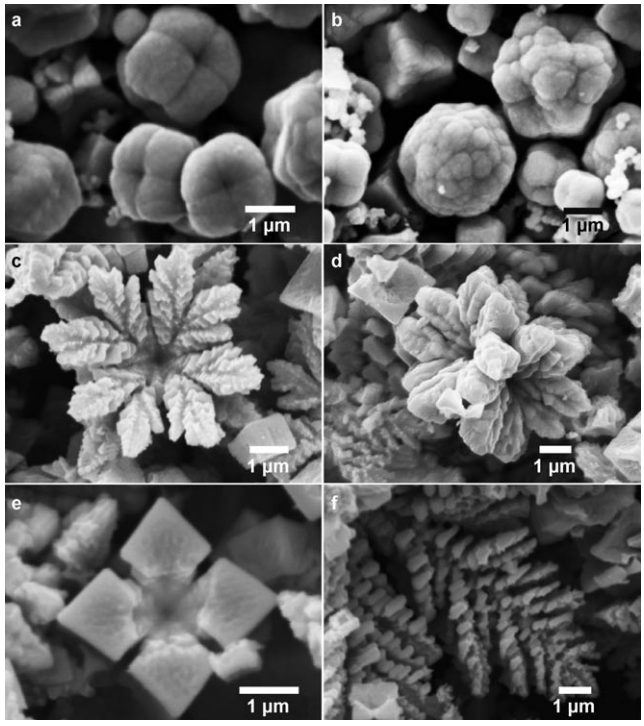

Figure 5. SEM images of PbS prepared through a hydrothermal reaction at 140 °C for 24 h with L-cysteine–Pb nanoarchitectures (a,b) or these nanoarchitectures dissolved in acetic acid as precursor (c–f).

spheres (Figure 5a,b) were composed of small dense particles. A few smaller PbS submicrometer spheres also existed in the powder.

To further understand the decomposition of the L-cysteine–Pb dandelion-like flowers, several adjustments to the experimental conditions were made. Micrometer-sized flowers and leaves of PbS were obtained by the hydrothermal method, but L-cysteine–Pb dandelion-like flowers were dissolved upon dropwise addition of acetic acid before the hydrothermal reaction. Most of these hierarchical structures were four- or eight-petaled flowers. Close examination of the images revealed that a typical eight-petaled flower (Figure 5c) was constructed by tight self-assembly of petals, and all these petals originated from the same core in a highly symmetric fashion. A dual-flower pattern with petals and pedicel conjugated together (Figure 5d) was also found in the PbS powder. Figure 5e depicts a typical four-petaled flower developed from the pedicel. In the formation of PbS flower structures, a leaflike hierarchical pattern of assembled nanorods (Figure 5f) also appeared, which consisted of many multiarmed nanorod-based structures arranged along a line and in parallel with each other. The leaflike structure has longer rods growing in the interior and shorter ones at the end.

In contrast with Figure 5, the products obtained by dissolving L-cysteine–Pb dandelion-like flowers in NaOH solution (1.0 M) at the beginning of the reaction were needle-like structures several hundreds of nanometers in diameter and some micrometers in length. The mechanism of the formation of highly ordered PbS flowers from the L-cysteine–Pb dandelion-like architectures remains a subject that requires further investigation.

In conclusion, we have demonstrated an extremely simple procedure for the shape-controlled and high-yield preparation of L-cysteine–Pb flowerlike architectures, assembled from well-aligned nanowires in a binary aqueous solution at room temperature. These novel and interesting architectures were used to fabricate semiconductor PbS with attractive morphologies under conventional hydrothermal conditions. The successful fabrication of nanoarchitectural morphologies not only provides an efficient route to the selectively controllable preparation of 3D architectures and 1D nanowires, but also provides new insights into the underlying mineralization mechanism of nano- and microarchitectures.

Experimental Section

In a typical procedure for preparing L-cysteine–Pb dandelion-like flowers, an aqueous solution of $Pb(OAc)_2$ (0.1 M, 0.25 mL) was injected into an aqueous solution of L-cysteine (0.01 M, 2.5 mL) at room temperature. After gentle shaking, the mixture turned gradually white and L-cysteine–Pb nanoarchitectures were formed.

In a surfactant-assisted synthesis, CTAB (0, 2.2, 3.3, or 4.4 mg) was dissolved in an aqueous solution of L-cysteine (0.01 M, 6 mL). The mixtures were heated to 50 °C and an aqueous solution of $Pb(OAc)_2$ (0.1 M, 0.6 mL) was added to form the products.

Decomposition of L-cysteine–Pb into PbS was carried out under conventional hydrothermal conditions. In a typical process, the white precipitate of L-cysteine–Pb was washed several times with pure water and mixed with the same volume of water. The mixture was then transferred into a Teflon-lined stainless-steel autoclave. After sealing, the autoclave was maintained at 140 °C for 24 h and then cooled to room temperature. The black product was collected by centrifugation at 3000 rpm for 2 min and washed three times with pure water and absolute ethanol. The sample was dried under vacuum at room temperature for characterization.

The concentration of lead was determined with a polarized Zeeman atomic-absorption spectrometer (model 180-80, Hitachi, Japan). The formation process of L-cysteine–Pb architectures was recorded with an optical microscope (XD-101, Jiangnan Optoelectrical Co., China) equipped with CCD camera (WV-GP470, Panasonic, Japan). The morphologies and microstructures of the products were characterized by SEM at 15.0 kV on an SS-550 microscope (Shimadzu, Japan) and by field-emission TEM at 200 kV with a Tecnai G2 F20 instrument (Philips, Holland). The XRD pattern was recorded with a D/max-2500 diffractometer (Rigaku, Japan) using $Cu_{K\alpha}$ radiation ($\lambda = 1.5418$ Å). FTIR spectra (4000–400 cm^{-1}) were recorded with a Magna-560 spectrometer (Nicolet, USA).

Received: June 6, 2007
Revised: July 4, 2007
Published online: August 23, 2007

Keywords: crystal growth · cysteine · lead · nanostructures · nanowires

[1] a) A. P. Alivisatos, *Science* **1996**, *271*, 933–937; b) M. A. El-Sayed, *Acc. Chem. Res.* **2001**, *34*, 257–264; c) J. T. Hu, T. W. Odom, C. M. Lieber, *Acc. Chem. Res.* **1999**, *32*, 435–445; d) J. Goldberger, R. Fan, P. D. Yang, *Acc. Chem. Res.* **2006**, *39*, 239–248.

[2] a) Z. L. Wang, *Adv. Mater.* **2003**, *15*, 432–436; b) Y. N. Xia, P. D. Yang, Y. G. Sun, Y. Y. Wu, B. Mayers, B. Gates, Y. D. Yin, F. Kim, H. Q. Yan, *Adv. Mater.* **2003**, *15*, 353–389.

[3] P. D. Yang, *Nature* **2003**, *425*, 243–244.

[4] a) F. Kim, S. Kwan, J. Akana, P. D. Yang, *J. Am. Chem. Soc.* **2001**, *123*, 4360–4361; b) T. Kuykendall, P. J. Pauzauskie, Y. F. Zhang, J. Goldberger, D. Sirbuly, J. Denlinger, P. D. Yang, *Nat. Mater.* **2004**, *3*, 524–528; c) D. M. Whang, S. Jin, Y. Wu, C. M. Lieber, *Nano Lett.* **2003**, *3*, 1255–1259; d) A. Tao, F. Kim, C. Hess, J. Goldberger, R. R. He, Y. G. Sun, Y. N. Xia, P. D. Yang, *Nano Lett.* **2003**, *3*, 1229–1233.

[5] a) B. Messer, J. H. Song, P. D. Yang, *J. Am. Chem. Soc.* **2000**, *122*, 10232–10233; b) Y. Huang, X. F. Duan, Q. Q. Wei, C. M. Lieber, *Science* **2001**, *291*, 630–633.

[6] X. F. Duan, Y. Huang, Y. Cui, J. F. Wang, C. M. Lieber, *Nature* **2001**, *409*, 66–69.

[7] N. A. Melosh, A. Boukai, F. Diana, B. Gerardot, A. Badolato, P. M. Petroff, J. R. Heath, *Science* **2003**, *300*, 112–115.

[8] B. P. Khanal, E. R. Zubarev, *Angew. Chem.* **2007**, *119*, 2245–2248; *Angew. Chem. Int. Ed.* **2007**, *46*, 2195–2198.

[9] R. Beckman, E. Johnston-Halperin, Y. Luo, J. E. Green, J. R. Heath, *Science* **2005**, *310*, 465–468.

[10] a) J. Aizenberg, D. A. Muller, J. L. Grazul, D. R. Hamann, *Science* **2003**, *299*, 1205–1208; b) C. B. Mao, D. J. Solis, B. D. Reiss, S. T. Kottmann, R. Y. Sweeney, A. Hayhurst, G. Georgiou, B. Iverson, A. M. Belcher, *Science* **2004**, *303*, 213–217; c) H. J. Liang, T. E. Angelini, P. V. Braun, G. C. L. Wong, *J. Am. Chem. Soc.* **2004**, *126*, 14157–14165; d) J. L. Zhang, J. M. Du, B. X. Han, Z. M. Liu, T. Jiang, Z. F. Zhang, *Angew. Chem.* **2006**, *118*, 1134–1137; *Angew. Chem. Int. Ed.* **2006**, *45*, 1116–1119.

[11] J. H. Gao, G. L. Liang, B. Zhang, Y. Kuang, X. X. Zhang, B. Xu, *J. Am. Chem. Soc.* **2007**, *129*, 1428–1433.

[12] H. Tong, Y. J. Zhu, L. X. Yang, L. Li, L. Zhang, *Angew. Chem.* **2006**, *118*, 7903–7906; *Angew. Chem. Int. Ed.* **2006**, *45*, 7739–7742.

[13] S. L. Xiong, B. J. Xi, C. M. Wang, G. F. Zou, L. F. Fei, W. Z. Wang, Y. T. Qian, *Chem. Eur. J.* **2007**, *13*, 3076 – 3081.
[14] B. Zhang, X. C. Ye, W. Y. Hou, Y. Zhao, Y. Xie, *J. Phys. Chem. B* **2006**, *110*, 8978 – 8985.
[15] Z. P. Zhang, X. Q. Shao, H. D. Yu, Y. B. Wang, M. Y. Han, *Chem. Mater.* **2005**, *17*, 332 – 336.
[16] J. Tang, A. P. Alivisatos, *Nano Lett.* **2006**, *6*, 2701 – 2706.
[17] a) M. Li, H. Schnablegger, S. Mann, *Nature* **1999**, *402*, 393 – 395; b) S. Kwan, F. Kim, J. Akana, P. D. Yang, *Chem. Commun.* **2001**, 447 – 448; c) A. Kameo, A. Suzuki, K. Torigoe, K. Esumi, *J. Colloid Interface Sci.* **2001**, *241*, 289 – 292; d) Y. Y. Yu, S. S. Chang, C. L. Lee, C. R. C. Wang, *J. Phys. Chem. B* **1997**, *101*, 6661 – 6664; e) C. J. Murphy, N. R. Jana, *Adv. Mater.* **2002**, *14*, 80 – 82.

